'Persistent currents' and eigenfunctions in microwave resonators with broken time-reversal symmetry

2002 J. Phys. A: Math. Gen. 35 4929

(http://iopscience.iop.org/0305-4470/35/23/309)

INSTITUTE OF PHYSICS PUBLISHING JOURNAL OF PHYSICS A: MATHEMATICAL AND GENERAL

J. Phys. A: Math. Gen. **35** (2002) 4929–4947 PII: S0305-4470(02)33292-X

'Persistent currents' and eigenfunctions in microwave resonators with broken time-reversal symmetry

Marko Vraničar[1], Michael Barth[2], Gregor Veble[1,3], Marko Robnik[1] and Hans-Jürgen Stöckmann[2]

[1] CAMTP Center for Applied Mathematics and Theoretical Physics, University of Maribor, Krekova 2, SI-2000 Maribor, Slovenia
[2] Fachbereich Physik, Philipps-Universität Marburg, Renthof 5, D-35032 Marburg, Germany

E-mail: mark.vranicar@uni-mb.si, michael.barth@physik.uni-marburg.de, gregor.veble@uni-mb.si, robnik@uni-mb.si and stoeckmann@physik.uni-marburg.de

Received 28 January 2002
Published 31 May 2002
Online at stacks.iop.org/JPhysA/35/4929

Abstract

A magnetic flux through a mesoscopic metallic ring gives rise to a persistent current which can be detected via characteristic oscillations of the magnetization depending on the applied field (Lévy *et al* 1990 *Phys. Rev. Lett.* **64** 2074). In this paper a direct visualization of such persistent currents in a microwave analogue experiment is reported, making use of the analogy between the probability density current in the quantum-mechanical system and the Poynting vector in the corresponding electromagnetic one. To break time-reversal symmetry, a small ring of a ferrite material in a static external magnetic field was introduced into the resonator. In our analysis of the experimental data we employ the off-diagonal elements of the scattering matrix. Due to the small size of the ferrite compared to the resonator size the symmetry was partially broken in the sense that the real and the imaginary parts of the wavefunctions are not equally large on average. The statistical properties of the wavefunction's real and imaginary parts $\mathrm{Re}(\psi)$, $\mathrm{Im}(\psi)$, respectively, as well as the distributions of the total wavefunction's amplitudes $|\psi|$ and the statistical properties of the probability density currents were also examined and compared to the theoretical predictions.

PACS numbers: 05.45.Mt, 03.65.−w, 03.65.Ge, 05.60.Gg, 73.23.Ra

[3] Present address: Center for the Study of Complex Systems (Dipartimento Scienze Chimiche Fisiche Matematiche), Università dell'Insubria, Via Valleggio 11, I-22100 Como, Italy.

1. Introduction

In a prism-shaped conducting resonator of thickness d the electric field vector of lowest frequency modes $\left(\nu < \frac{c_0}{2d}\right)$ reduces to a single component E_z perpendicular to the planar base which also reduces the electromagnetic vector field wave equation to a simple scalar Helmholtz equation, with the Dirichlet boundary condition for E_z. When the planar base of the resonator has the shape of a two-dimensional billiard the same Helmholtz equation also represents the stationary Schrödinger equation for a free point particle enclosed in the two-dimensional domain. This formal analogy between the component E_z and the billiard particle wavefunction ψ is the key to experimental studies of quantum chaos with microwaves on a 10 cm scale (Stöckmann and Stein 1990). In the last decade the analogy has been used many times to study spectra and wavefunctions of numerous billiard systems, and an excellent qualitative and quantitative agreement between the experiment and the theory has been reported (see, e.g., Rehfeld *et al* 1999, Veble *et al* 2000). For reviews and further reading the reader is referred to the book by Stöckmann (1999) and papers by Richter (1999) and Sridhar (2000).

The goal of this work is to experimentally study wavefunctions and currents in quantum billiards with broken time-reversal symmetry, corresponding to a bound state version of the Aharonov–Bohm effect (Aharonov and Bohm 1959, Berry and Robnik 1986a, 1986b, Narevich *et al* 2001). While the time-reversal symmetry (TRS) is easily broken in charged particle billiards even when a single external magnetic flux line is applied, this is not so in microwave resonators. In this case the analogy between the quantum billiards and the microwave resonators needs to be reconsidered. To overcome that problem we follow the work of So *et al* (1995), Stoffregen *et al* (1995), Haake *et al* (1996) and Wu *et al* (1998) where the effect of an external magnetic field on a charged particle was simulated by inserting a piece of a ferrite material in an external static magnetic field into the microwave resonator. In two of these works a bow-tie-shaped billiard with the flat boundary completely covered by the ferrite layer was used to study spectral statistics (So *et al* 1995), the wavefunction's probability density distribution and the two-point probability density correlation function (Wu *et al* 1998) in the semiclassical regime. A good agreement with the universally predicted statistical measures of GUE was reported in both cases: so it is reasonable to believe that the complete TRS breaking was achieved in the semiclassical regime.

Since in our experiment both modulus and phase of the wavefunctions are determined, it is easy to reconstruct the Poynting vector at any point within the resonator (Šeba *et al* 1999). This is the key to the visualization of 'persistent currents' in microwave resonators with broken TRS, having a direct analogy to the persistent currents observed by Lévy *et al* (1990) in mesoscopic copper rings (see Mohanty (1999) for a recent review). Of course in a microwave resonator the currents are not 'persistent' in the true sense of the word because of the unavoidable absorption in the walls, hence the quotation marks.

The billiards used are two representatives of the so-called quadratic billiard family (Robnik 1983, 1984) with linear dimensions of about 250 mm. They are obtained by a conformal mapping of the unit circle with one free parameter (see section 3). TRS is broken by introducing a small ferrite ring with a diameter of 22 mm and a thickness of 1 mm. Due to the small relative size of the ferrite only a partial TRS breaking effect is expected. The word partial here means that the real and imaginary parts of a complex wavefunction are not of the same size on average, but that

$$\langle \mathrm{Im}^2(\psi)\rangle < \langle \mathrm{Re}^2(\psi)\rangle. \tag{1}$$

In this case we cannot speak about GOE or GUE universality classes, but about an intermediate class of systems with partially broken TRS instead, when statistical measures of probability density $|\psi|^2$ and wavefunction amplitude $|\psi|$ are considered.

However, our experimental approach as described in section 3 is different from that used by Wu *et al* (1998) enabling us to study the complete wavefunction, namely the amplitude and the quantum phase that can be further used to compute persistent probability density currents of a system with (partially) broken TRS. Since the imaginary part $\mathrm{Im}(\psi)$ itself and the probability density currents are the leading order effect of the ferrite perturbation, universalities are believed to be found in statistical properties of these two quantities even in the case of partially broken TRS (Saichev *et al* 2002).

In section 2 we discuss the experimental method and set-up we use and briefly explain the effect of the ferrite. The quadratic billiard family is defined in section 3. In section 4 we show and comment on our experimental results on structures and statistical measures of eigenstate wavefunctions and persistent currents in the billiards with broken TRS. Section 5 is devoted to a summary and conclusions.

2. Experimental method and set-up

The complete information about the billiard eigenfunctions and spectrum is contained in the billiard Green function

$$G(\boldsymbol{r}_i, \boldsymbol{r}_j, E) = \sum_n \frac{\psi_n(\boldsymbol{r}_i)\psi_n(\boldsymbol{r}_j)^*}{E_n - E}. \tag{2}$$

To study billiards or equivalently resonators experimentally antennas are attached to the observed resonator in order to bring the microwaves into the resonator and to measure the resonator's response. The Green function is not directly accessible in a microwave experiment; however, the scattering matrix $\mathcal{S}$ connects the vector $\boldsymbol{a}$ of the microwave amplitudes entering the resonator through the set of antennas to the vector $\boldsymbol{b}$ of microwave amplitudes leaving the resonator (through the same antennas) via the simple linear relation

$$\boldsymbol{b} = \mathcal{S}\boldsymbol{a}. \tag{3}$$

In case of two antennas or channels attached, which is the set-up we use, $\boldsymbol{a}$ and $\boldsymbol{b}$ are two-dimensional vectors and $\mathcal{S}$ is a 2×2 matrix.

So, to start with we have to relate the Green function (2) of a closed billiard to the measured scattering matrix $\mathcal{S}$ of the system with antennas attached at different positions $\boldsymbol{r}_i$. As shown by Stein *et al* (1995) (see also Stöckmann (1999)) the relation reads

$$\mathcal{S} = (1 + \alpha^* G)^{-1}(1 + \alpha G) \qquad G_{i,j} = G(\boldsymbol{r}_i, \boldsymbol{r}_j, E). \tag{4}$$

Here α is a complex parameter determining the coupling of the resonator with the antennas at positions $\boldsymbol{r}_i$; α depends on the shape and the size of the antennas, and on the microwave frequency. In general, if the N antennas are different so that their couplings are different as well, α should be replaced by the diagonal matrix $\underline{\underline{\alpha}} = \mathrm{diag}(\alpha_1, \alpha_2, \ldots, \alpha_N)$ appearing in equation (4) on the rhs of the matrix G, with α_i being the coupling parameter of the ith antenna. But this does not change the shape of the $\mathcal{S}$ matrix elements and for the sake of simplicity we write our formulae in terms of a single coupling parameter α.

In the vicinity of a single resonance the Green function matrix $G_{i,j}$ is dominated by a single term of the sum (2), and the scattering matrix (4) simplifies to

$$\mathcal{S} = 1 + 2\mathrm{i}\ \mathrm{Im}(\alpha)\mathcal{G} \tag{5}$$

where $\mathcal{G}$ is the modified Green function

$$\mathcal{G}(\boldsymbol{r}_i, \boldsymbol{r}_j, E) = \frac{\psi_n(\boldsymbol{r}_i)\psi_n(\boldsymbol{r}_j)^*}{E_n - E + \Delta_n - \mathrm{i}\Gamma_n} \tag{6}$$

in the vicinity of the nth resonance, complexly shifted by

$$\Delta_n = \mathrm{Re}(\alpha) \sum_i |\psi_n(\boldsymbol{r}_i)|^2 \tag{7}$$

in the real direction and by

$$\Gamma_n = \mathrm{Im}(\alpha) \sum_i |\psi_n(\boldsymbol{r}_i)|^2 \tag{8}$$

in the imaginary direction due to the coupling of the resonator with the antennas. The resonant positions are thus shifted by Δ_n and broadened by Γ_n. For only one antenna the shift and the width of the resonances at a given position are directly proportional to the wavefunction's probability density at that position which offers one possibility to measure the eigenfrequency and the probability density used by Sridhar *et al* (1992) and Wu *et al* (1998).

In the present experiment we use two antennas. The first one is a thin wire used as an emitting and receiving antenna and is moved across the whole billiard domain, while the other one is a wire with teflon coating for stronger coupling and is kept fixed at position $\boldsymbol{r}_2$ serving only as a receiving antenna. In this way we measure the $\mathcal{S}_{1,1}$ and $\mathcal{S}_{2,1}$ matrix elements as functions of the microwave frequency and position $\boldsymbol{r}_1$ of the moving antenna. Using a vector network analyser Agilent 8720ES we are able to measure the complete complex signal including the intensity of the signal and its phase relative to the incoming reference wave. The complex signal is then analysed at each measured spatial position by fitting it close to a resonance with the function

$$\tilde{\mathcal{S}}(\nu) = \frac{x_1 + \mathrm{i}x_2}{x_3 - \nu^2 - \mathrm{i}x_4} + \text{background} \tag{9}$$

where x_1, x_2, x_3 and x_4 are the real fit parameters and ν is the microwave frequency; for the background we take a linear function. Comparing equation (9) with equations (5) and (6) for the scattering matrix elements it can be seen that in case of the $\mathcal{S}_{1,1}$ signal

$$x_1(\boldsymbol{r}_1) + \mathrm{i}x_2(\boldsymbol{r}_1) \propto |\psi(\boldsymbol{r}_1)|^2 \tag{10}$$

while in case of the $\mathcal{S}_{2,1}$ signal

$$x_1(\boldsymbol{r}_1) + \mathrm{i}x_2(\boldsymbol{r}_1) \propto \psi(\boldsymbol{r}_1)^* \tag{11}$$

where the proportionality factor may be complex due to the unknown but position-independent experimental phase and the phase of ψ at the position of the fixed antenna $\boldsymbol{r}_2$. It is also evident that in both cases $x_3 \propto E_n + \Delta_n$ and $x_4 \propto \Gamma_n$.

Despite the fact that a slightly more standard approach is to analyse the $\mathcal{S}_{1,1}$ signal we see two advantages of using the $\mathcal{S}_{2,1}$ signal when dealing with systems without time-reversal invariance and thus with complex wavefunctions. First, we can get both real and imaginary parts of the billiard wavefunctions when $\mathcal{S}_{2,1}$ is fitted as can be seen from (11), while $\mathcal{S}_{1,1}$ only yields the wavefunction's probability density. Second, for complex wavefunctions real and imaginary parts can be obtained with a much higher accuracy from $\mathcal{S}_{2,1}$ for the following reason. The complex wavefunctions do not possess nodal lines but only discrete nodal points which is also reflected in the distribution of the wavefunction amplitude $|\psi|$ which drops to zero as $|\psi| \to 0$ in contrast to the systems with TRS and real wavefunctions, where it is finite (non-vanishing) at $|\psi| = 0$. For this reason it is important to measure wavefunctions at small values of $|\psi|$ (when compared to $\frac{1}{\sqrt{A}}$, where A is the billiard area) as accurately as possible

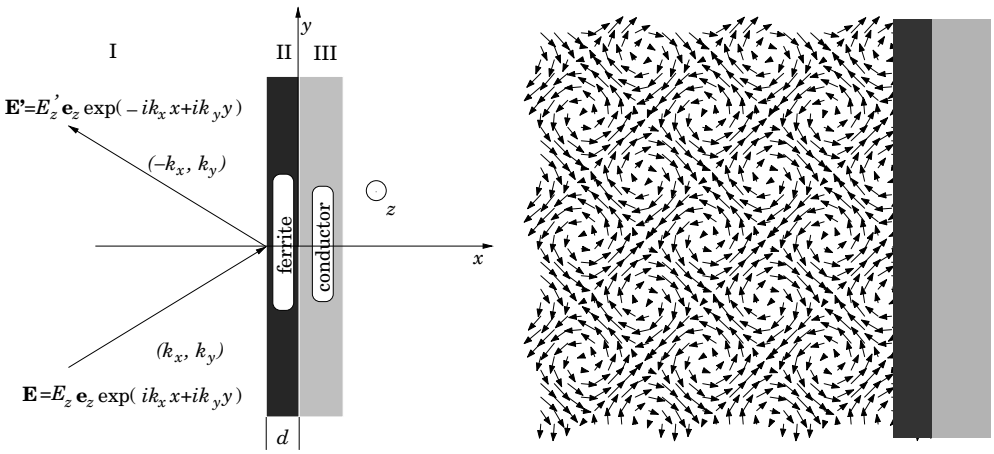

Figure 1. Reflection from the ferrite layer (left). Poynting vector after reflection of a plane wave $E_z \propto \exp(\mathrm{i}k_x x)\sin(k_y y)$ from the ferrite layer (right).

in order to observe the statistical and qualitative difference in amplitudes $|\psi|$ of complex and real wavefunctions. Since the $\mathcal{S}_{2,1}$ signal is proportional to ψ the signal-to-noise ratio at small amplitudes is better in the $\mathcal{S}_{2,1}$ than in the $\mathcal{S}_{1,1}$ signal as the latter is proportional to $|\psi|^2$.

As mentioned in the introduction the time-reversal symmetry of microwave resonators is broken by inserting a piece of a ferrite material in an external static magnetic field into the resonator domain. A ferrite is a material with non-vanishing spontaneous magnetization M_0 and a large resistivity and so it can be treated as a lossless dielectric. When such a ferrite is put into the thin microwave resonator and an additional external static magnetic field H_0 is applied perpendicular to the plane of the resonator base the effective permeability tensor felt by the microwave magnetic field lying in the plane of the base, in the absence of the microwave absorption, reads

$$\underline{\underline{\mu}} = \begin{pmatrix} \mu & -\mathrm{i}\kappa & 0 \\ \mathrm{i}\kappa & \mu & 0 \\ 0 & 0 & 1 \end{pmatrix} \qquad \mu = 1 + \frac{\omega_0\omega_M}{\omega_0^2 - \omega^2} \quad \kappa = -\frac{\omega\omega_M}{\omega_0^2 - \omega^2} \tag{12}$$

where $\omega_M = \gamma_{\mathrm{eff}} M_0$, $\omega_0 = \gamma_{\mathrm{eff}} H_0$ and γ_{eff} is the effective gyromagnetic ratio of the electrons in the ferrite (So *et al* 1995, Stöckmann 1999). For further reading and more realistic models of ferrite materials please see the books by Soohoo (1960), and Lax and Button (1962).

Due to the non-vanishing purely imaginary off-diagonal elements of the tensor $\underline{\underline{\mu}}$ the phase of the wave reflected from the ferrite depends on the direction of the incident wave which is clearly a TRS breaking effect. To demonstrate the ferrite boundary reflection effect (for more details see Schanze *et al* (2002)) we consider the simple situation of a plane electromagnetic wave

$$\boldsymbol{E}^0 = E_z^0 \boldsymbol{e}_z \exp(\mathrm{i}k_x x + \mathrm{i}k_y y)\exp(-\mathrm{i}\omega t) \qquad \boldsymbol{H}^0 = -\frac{\mathrm{i}}{\omega\mu_o}\nabla \times \boldsymbol{E}^0 \tag{13}$$

coming from the left ($x < 0$) and being reflected from the ferrite layer of thickness d carried by the infinite conducting plate at $x = 0$ as is sketched in figure 1 (left). Imposing the boundary conditions

$$\boldsymbol{E}_{\parallel}^{I}\big|_{x=-d} = \boldsymbol{E}_{\parallel}^{II}\big|_{x=-d} \qquad \boldsymbol{E}_{\parallel}^{II}\big|_{x=0} = 0 \tag{14}$$

and

$$\boldsymbol{H}_{\parallel}^{I}\big|_{x=-d} = \boldsymbol{H}_{\parallel}^{II}\big|_{x=-d} \tag{15}$$

and taking into account the form (12) of the tensor $\underline{\underline{\mu}}$ we get the reflection coefficient

$$r = \exp(-2\mathrm{i}k_x d)\frac{\sin(K_x d) - \mathrm{i}\left[\frac{\mu}{\mu^2-\kappa^2}\frac{K_x}{k_x}\cos(K_x d) + \underline{\frac{\kappa}{\mu^2-\kappa^2}\frac{k_y}{k_x}\sin(K_x d)}\right]}{\sin(K_x d) + \mathrm{i}\left[\frac{\mu}{\mu^2-\kappa^2}\frac{K_x}{k_x}\cos(K_x d) + \underline{\frac{\kappa}{\mu^2-\kappa^2}\frac{k_y}{k_x}\sin(K_x d)}\right]}$$
$$= \exp(\mathrm{i}\theta(k_y)) \tag{16}$$

where $K_x = \sqrt{k^2\frac{\mu^2-\kappa^2}{\mu} - k_y^2}$. As we can see from (16) the phase $\theta(k_y)$ depends on the sign of k_y due to the underlined terms in (16) yielding a non-vanishing stationary (meaning time-averaged) Poynting vector

$$\langle \boldsymbol{P}\rangle_t = \langle \mathrm{Re}(\boldsymbol{E}) \times \mathrm{Re}(\boldsymbol{H})\rangle_t \tag{17}$$

even if the incident wave is of the form

$$\boldsymbol{E}^0 = E_z^0 \boldsymbol{e}_z \exp(\mathrm{i}k_x x)\sin(k_y y)\exp(-\mathrm{i}\omega t). \tag{18}$$

In the particular case of the one-component microwave electric field occurring in low frequency modes of thin resonators and in our demonstrative example (18) the Poynting vector (17) reduces to

$$\langle \boldsymbol{P}\rangle_t = \frac{c\epsilon_0}{2k}\mathrm{Im}(E_z^*\nabla E_z). \tag{19}$$

For the incident wave from equation (18), $\langle \boldsymbol{P}\rangle_t$ can be expressed as

$$\langle \boldsymbol{P}\rangle_t = \frac{c\epsilon_0}{2k}\left(E_z^0\right)^2\left(-\boldsymbol{e}_x k_x \sin\left(\frac{\Delta\theta}{2}\right)\sin\left(2k_y y + \frac{\Delta\theta}{2}\right) + \boldsymbol{e}_y k_y \sin\left(\frac{\Delta\theta}{2}\right)\sin(2k_x x - \bar{\theta})\right) \tag{20}$$

with

$$\Delta\theta = \theta(k_y) - \theta(-k_y) \qquad \bar{\theta} = \frac{\theta(k_y) + \theta(-k_y)}{2}.$$

The current pattern resulting from equation (20) is plotted in figure 1 (right).

Please note the one-to-one correspondence between the Poynting vector (19) and the quantum-mechanical probability density current

$$\boldsymbol{j} = \frac{\hbar}{m}\mathrm{Im}(\psi^*\nabla\psi) \tag{21}$$

enabling us to experimentally study the latter with microwave resonators.

Figure 1 (right) clearly reflects the general feature of complex wavefunctions, namely the non-vanishing probability density current arranged in vortex structures with vortex centres at the wavefunction's nodal points where the quantum phase is not defined.

3. The billiard systems under study

The billiard systems used in the experiments are the two representatives of the so-called quadratic (also named Robnik) billiard family. The domain of the two-dimensional quadratic billiards is defined by the complex conformal mapping

$$w(z) = z + \lambda z^2 \qquad w = x + \mathrm{i}y \qquad z = x' + \mathrm{i}y' \qquad |z| \leqslant 1 \tag{22}$$

of a unit disc in a complex z plane onto the complex w plane (Robnik 1983, 1984). The billiard boundary is analytic for all values of λ from the interval $[0, 0.5)$. Changing the boundary deformation parameter from 0 (unit circle) to 0.5 (cardioïd) the classical dynamics traverses all kinds of qualitative behaviour. Namely, at $\lambda = 0$ the dynamics is integrable, for $\lambda \leqslant 0.25$ it is of a mixed type, while at $\lambda = 0.25$ the boundary becomes non-convex and the dynamics is almost chaotic with tiny stability islands. As recently shown by Dullin and Bäcker (2001) the stability islands may exist up to any $\lambda < 0.5$ but their relative volume in the available phase-space is so small that the billiards for $\lambda > 0.2791$ may be considered as fully chaotic for practical purposes which is also supported by strong numerical evidence (Li and Robnik 1994b). However, it was rigorously proven by Markarian (1993) that at $\lambda = 0.5$ the quadratic billiard is ergodic.

In the experiment the $\lambda = 0.15$ and $\lambda = 0.4$ quadratic billiards were studied. The first one is classically of a mixed type while the second one is considered chaotic. The resonators were cut out of a brass plate up to a depth of 8 mm, of the shape of the above mentioned billiards. The linear scales of the resonators were 127 mm and 114 mm per unit of billiard length in the definition (22), respectively. In both cases a ferrite ring, 22 mm in diameter, and $\gamma_{\mathrm{eff}} = 2.01$ in units of the Bohr magneton was inserted into the resonator interiors and an external magnetic field of about 140 mT was applied determining the resonant frequency of the ferrite at $\omega_0 \approx 2\pi \times 4$ GHz. The moving antenna was moved in 5 mm steps across the rectangular grid in the resonator domain. The ferrite was placed away from the reflection symmetry line in order to avoid the false TRS breaking due to the existence of the antiunitary symmetry combined by the time inversion and the mirror reflection transformations as discussed by Robnik and Berry (1986) and Robnik (1986).

The reason to use such a relatively small amount of the ferrite (compared to the resonator area) is to diminish the relative effect of the microwave absorption in the ferrite with respect to the desired boundary reflection effect. Since the principle of the electronic paramagnetic resonance is essential to break TRS, absorption is unavoidable, with the disturbing consequence that it drives us away from the closed billiard system with broken TRS we want to study in the first place. However, we shall see in the next section that there are resonances with negligible or at least non-dominant absorption in the frequency range 3–5 GHz. At the same time, since the size of the ferrite is small compared to the wavelength which close to the ferrite resonance frequency ($\omega_0 \approx 2\pi \times 4$ GHz) is $\approx$75 mm, we are able to study the transition regime between the two universality classes of GOE and GUE where the partial breaking of TRS should occur due to the fact that at the wavelength of $\approx$75 mm we are far below the semiclassical limit. To our knowledge the transition regime where the wavefunctions are complex-valued but their real and imaginary parts are of different strengths has not been experimentally studied yet in the context of closed systems but only in the context of partially open systems (see Šeba *et al* 1997).

4. Results

Resonances of both billiards were analysed in the frequency interval [3 GHz, 5 GHz] in the neighbourhood of the ferrite paramagnetic resonant frequency $\nu_0 = \frac{\omega_0}{2\pi} = 4$ GHz. Apart from the absorption in the ferrite and the walls, which will be discussed later on, the billiard systems are closed. To obtain the eigenstate wavefunctions, $\mathcal{S}_{2,1}$ was analysed as described in section 2 yielding the eigenstate wavefunctions

$$\psi'(x, y) = p(x, y) + \mathrm{i}q(x, y) \tag{23}$$

multiplied by an unknown phase factor $\exp(\mathrm{i}\phi)$. In this form the wavefunction's real and imaginary parts are not necessarily statistically independent, i.e. they are not orthogonal

$$\int_A p(x, y)q(x, y)\,\mathrm{d}S \neq 0 \tag{24}$$

where A is the billiard area. In order to remove the correlation between the real and imaginary parts, (23) should be multiplied by a phase factor

$$\psi(x, y) = \exp(-\mathrm{i}\phi)(p(x, y) + \mathrm{i}q(x, y)) \tag{25}$$

determined by the condition

$$\int_A \mathrm{Re}(\psi(x, y))\,\mathrm{Im}(\psi(x, y))\,\mathrm{d}S = 0 \tag{26}$$

which gives us

$$\tan(2\phi) = \frac{2\langle pq\rangle}{\langle p^2\rangle - \langle q^2\rangle} \tag{27}$$

with

$$\begin{aligned} \langle pq\rangle &= \frac{1}{A}\int_A p(x, y)q(x, y)\,\mathrm{d}S \qquad \langle p^2\rangle = \frac{1}{A}\int_A p^2(x, y)\,\mathrm{d}S \\ \langle q^2\rangle &= \frac{1}{A}\int_A q^2(x, y)\,\mathrm{d}S. \end{aligned} \tag{28}$$

Equation (27) has infinitely many solutions, differing, however, only in an irrelevant global phase rotation. Therefore the phase ϕ is further specified such that

$$\frac{\langle \mathrm{Im}^2(\psi)\rangle}{\langle \mathrm{Re}^2(\psi)\rangle} = \gamma^2 \leqslant 1. \tag{29}$$

Please note that in cases of partially broken TRS where $\langle \mathrm{Im}^2(\psi)\rangle < \langle \mathrm{Re}^2(\psi)\rangle$ the transformation (25) is necessary in order to see the structural difference of a wavefunction's real and imaginary parts.

To reduce the noise the wavefunctions are transformed to the k-space using the fast Fourier transform where they are slightly filtered by the low pass frequency filter of the Gaussian form

$$F(k) = \exp\left(-\frac{k^2}{(3k_0)^2}\right) \tag{30}$$

where k_0 is the wavenumber of the eigenstate. A Lorentzian filter can also be used instead of the Gaussian since the results are independent of the form of filter as they should be.

The gradients of the wavefunctions entering the expression for probability density currents (21) are also calculated in the k-space instead of approximating them in the configuration space by differences. The gradients as well as the wavefunctions themselves are then transformed back to the configuration space using the inverse fast Fourier transform.

Since we are dealing with chaotic ($\lambda = 0.4$) and mixed-type ($\lambda = 0.15$) billiards our ambition is not only to observe the qualitative features of systems with broken TRS but also to test some statistical measures predicted by the theory of quantum chaos. In this context the key result is the conjecture of Berry (1977) that the wavefunctions of classically chaotic systems with TRS in the semiclassical limit follow the Gaussian distribution

$$P(x) = \frac{1}{\sqrt{2\pi}}\exp\left(-\frac{x^2}{2}\right) \qquad x = \frac{\psi}{\sqrt{\langle\psi^2\rangle}} \tag{31}$$

as they are sampled at different positions in the corresponding configuration space. Berry's conjecture has been numerically and experimentally tested by so many authors in the past that

we cannot quote them all here. However, it should be mentioned that McDonald and Kaufman (1979, 1988) were among the first to confirm the validity of the distribution (31), and another recent numerical verification of high statistical significance was published in Li and Robnik (1994a). The implications of Berry's conjecture on current and vortex distributions have been studied numerically by Saichev *et al* (2002) in a series of papers, and experimentally by Barth and Stöckmann (2002), partly in the same systems presented in the present work.

If the TRS of a classically chaotic system is perturbed by an external magnetic field or a magnetized ferrite, the real eigenstates of the unperturbed system are complexly mixed suggesting that the real and imaginary parts of the newly formed wavefunctions separately follow independent Gaussian distributions (31). Based on this assumption several other statistical measures concerning classically chaotic systems with broken TRS have been derived. The two of them studied in this work are the wavefunction amplitude $|\psi|$ distribution

$$P(y,\delta) = \frac{2y}{\delta}\exp\left(-\frac{y^2}{\delta^2}\right) I_0\left(y^2\frac{\sqrt{1-\delta^2}}{\delta^2}\right) \qquad y = \frac{|\psi|}{\sqrt{\langle|\psi|^2\rangle}} \qquad \delta = \frac{2\gamma}{\gamma^2+1} \tag{32}$$

where γ is the TRS breaking parameter defined in (29) and I_0 is the modified zeroth order Bessel function of the first kind (for the distribution of $|\psi|^2$ see Kanzieper and Freilikher (1996), Šeba *et al* (1997), Saichev *et al* (2002)), and the absolute probability density current distribution

$$P(z) = 4zK_0(2z) \qquad z = \frac{j}{\sqrt{\langle j^2\rangle}} \qquad j = \sqrt{j_x^2 + j_y^2} \tag{33}$$

where K_0 is the modified zeroth order Bessel function of the second kind (Saichev *et al* 2002). Since the existence of the non-vanishing probability density currents is the leading order effect of the TRS breaking perturbation, the distribution (33) is independent of δ and thus universal while (32) ranges with δ between the two known limiting distributions

$$P^{\mathrm{GOE}}(y) = P(y,0) = \sqrt{\frac{2}{\pi}}\exp\left(-\frac{y^2}{2}\right) \tag{34}$$

for the GOE class ($\gamma = \delta = 0$) and

$$P^{\mathrm{GUE}}(y) = P(y,1) = 2y\exp\left(-y^2\right) \tag{35}$$

in the case of the GUE class ($\gamma = \delta = 1$).

Our experimental results for selected eigenstates of the chaotic $\lambda = 0.4$ billiard with the ferrite ring attached are plotted in figures 2–4, while in figures 5 and 6 we present our results for the $\lambda = 0.15$ classically KAM billiard. In the upper parts of the figures we show the wavefunction's real part, imaginary part and the amplitude contour plots respectively. The greyness of the billiard points $\boldsymbol{r}_i$ in $\mathrm{Re}(\psi(\boldsymbol{r}_i))$ and $\mathrm{Im}(\psi(\boldsymbol{r}_i))$ plots is determined with respect to the greyness function

$$g^f(\boldsymbol{r}_i) = \frac{1}{2}\left(1 - \frac{f(\boldsymbol{r}_i)}{|f|_{\max}}\right) \qquad |f|_{\max} = \max_j\{|f(\boldsymbol{r}_j)|\}$$
$$f(\boldsymbol{r}_i) = \mathrm{Re}(\psi(\boldsymbol{r}_i)),\ \mathrm{Im}(\psi(\boldsymbol{r}_i)) \tag{36}$$

where $g = 1$ determines 'white' greyness (appearing at $f = -|f|_{\max}$) while $g = 0$ means 'black' greyness level (appearing at $f = -|f|_{\max}$). In the same plots the contours are equally spaced and set to values

$$c_n = |f|_{\max}\frac{(-9+2n)}{10} \qquad n = 0,\ldots,9. \tag{37}$$

The amplitude $|\psi|$ is plotted with 10 equally spaced contours between 0 (white) and $\max_j\{|\psi|\}$ (black greyness level).

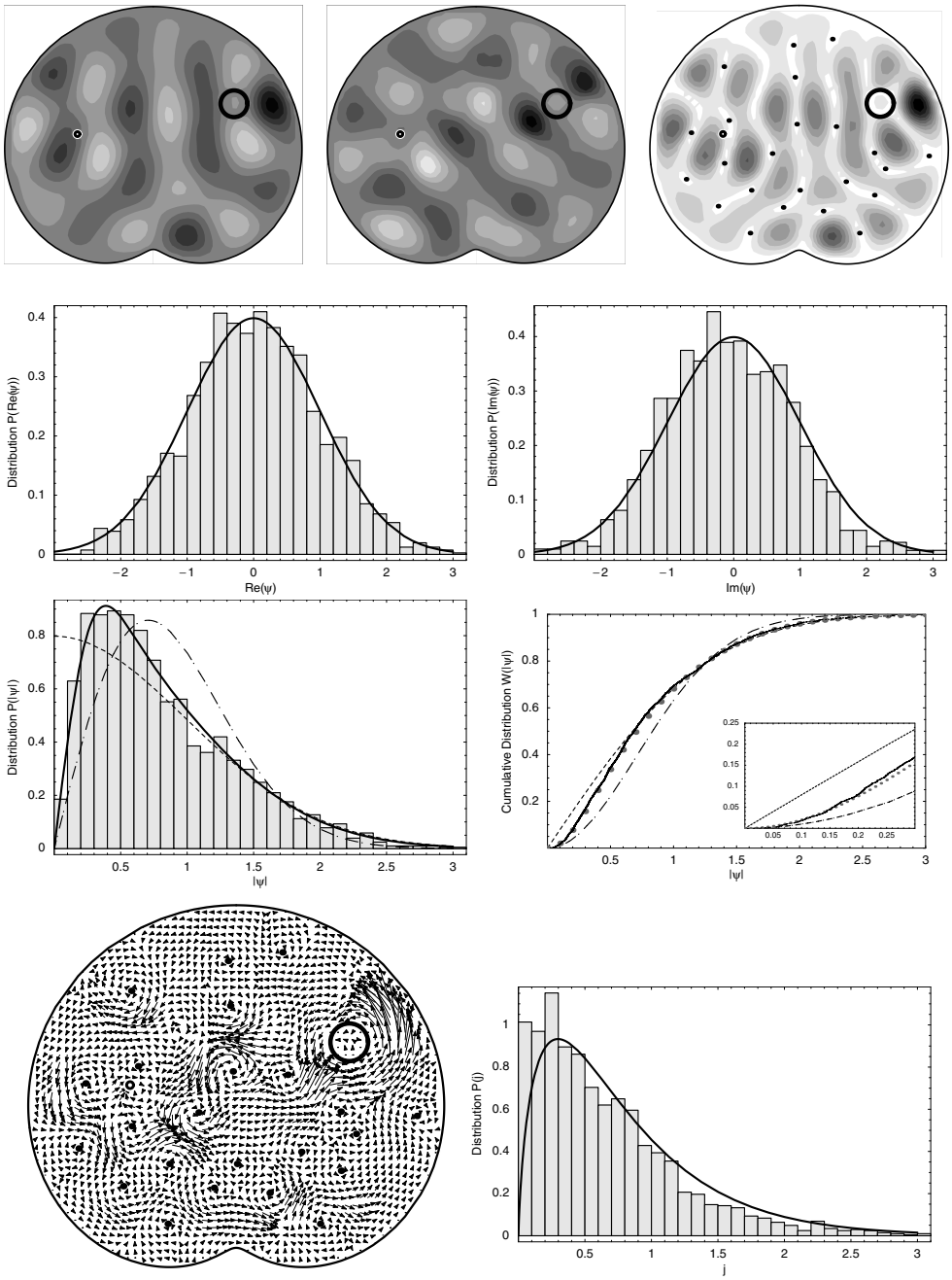

Figure 2. In the upper part we show $\mathrm{Re}(\psi)$, $\mathrm{Im}(\psi)$ and $|\psi|$ of the $\lambda = 0.4$ billiard eigenstate corresponding to the $\nu \approx 4.50$ GHz with $\gamma = 0.254$ ($\delta = 0.477$). For the definition of the greyness levels and the contour values, please see equations (36) and (37), and the text. Distributions of $\mathrm{Re}(\psi)$, $\mathrm{Im}(\psi)$ and $|\psi|$ and the cumulative distribution of $|\psi|$ are presented in the middle part together with the theoretical predictions (full thick line in the case of histograms and grey bullets for the cumulative distribution). The universal limiting distributions of $|\psi|$ are also drawn with the dashed line for GOE and dashed-dotted line for GUE. The probability density current and its absolute value distribution are shown in the lower part. Black bullets in the upper right and lower left parts mark some amplitude nodal points and current vortices.

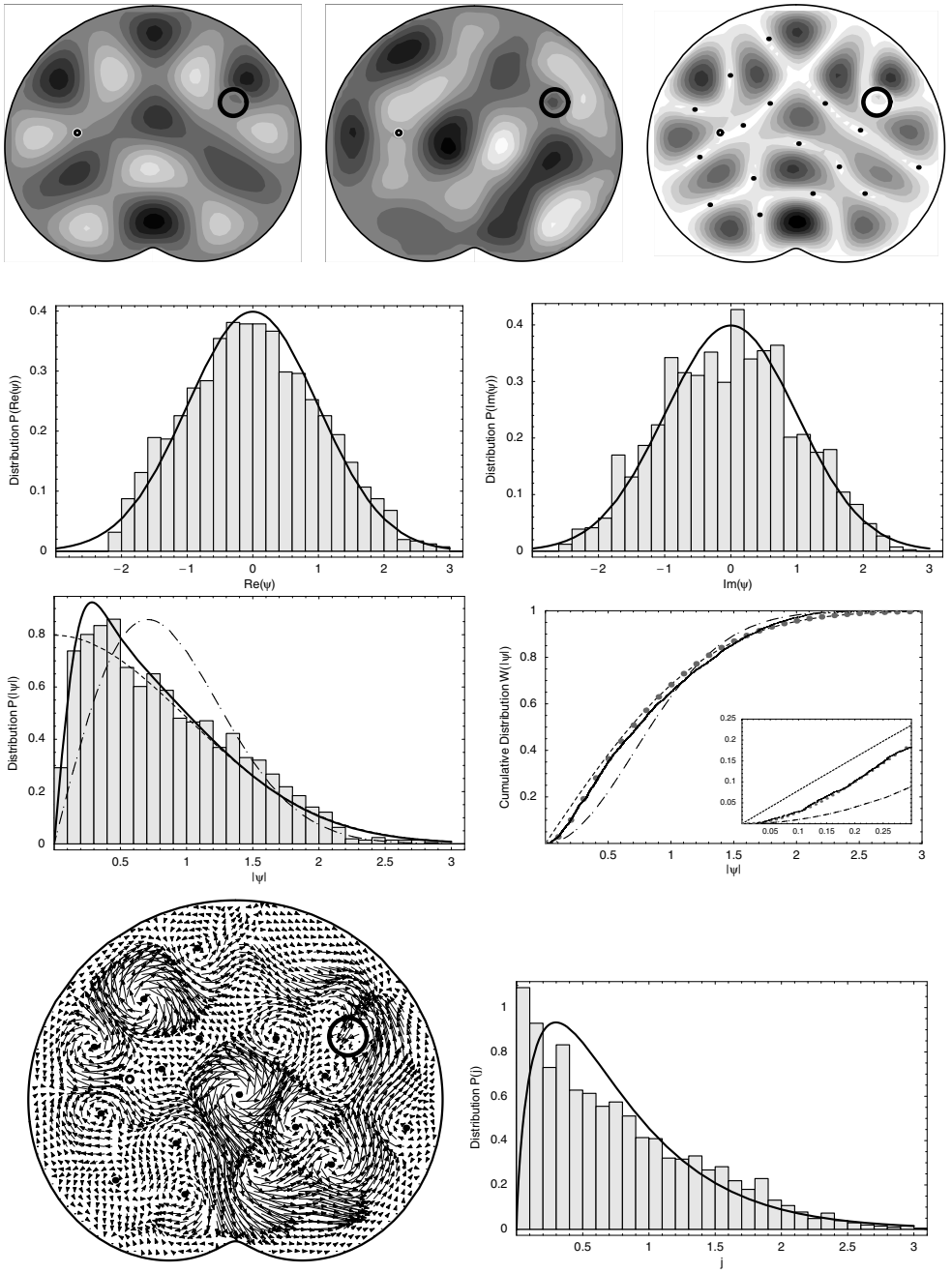

Figure 3. Same as figure 2 but for the billiard eigenstate at $\nu \approx 3.62$ GHz with $\gamma = 0.174$ ($\delta = 0.338$).

The wavefunction statistics follow in the middle segments of the figures. Here we plot the distributions of $\mathrm{Re}(\psi)$, $\mathrm{Im}(\psi)$, $|\psi|$ and the cumulative (integrated) distributions of $|\psi|$ in this order. In the lower parts of the figures we show the probability density currents (Poynting

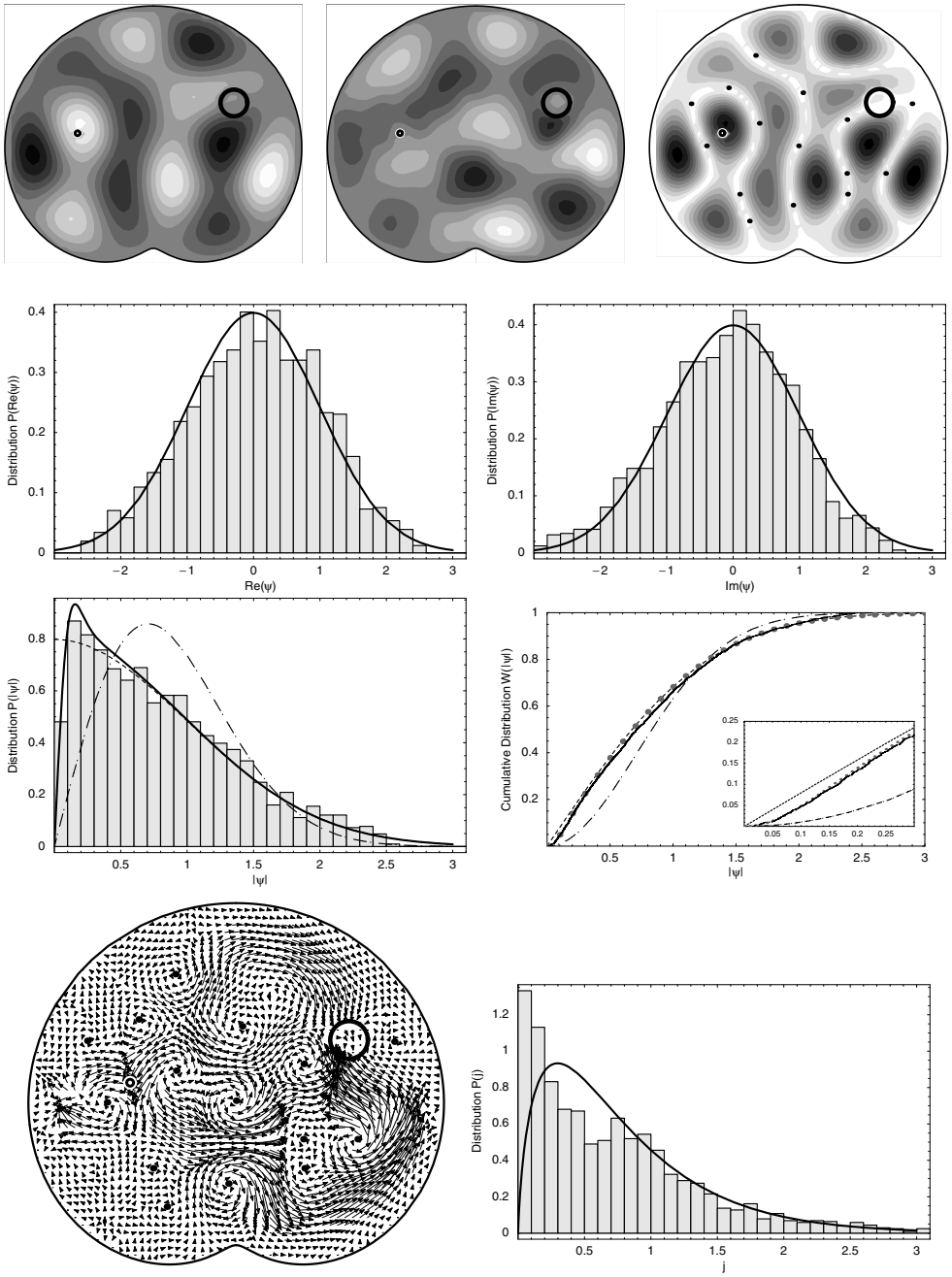

Figure 4. Same as figure 2 but for the billiard eigenstate at $\nu \approx 3.45$ GHz with $\gamma = 0.090$ ($\delta = 0.179$).

vectors) as well as the distributions of absolute current values $j = \sqrt{j_x^2 + j_y^2}$. The number of statistical objects is given by the number of applied antenna positions, i.e. 2060 for the $\lambda = 0.4$ billiard and 2045 for the $\lambda = 0.15$ billiard. All distributions displayed are normalized to a total

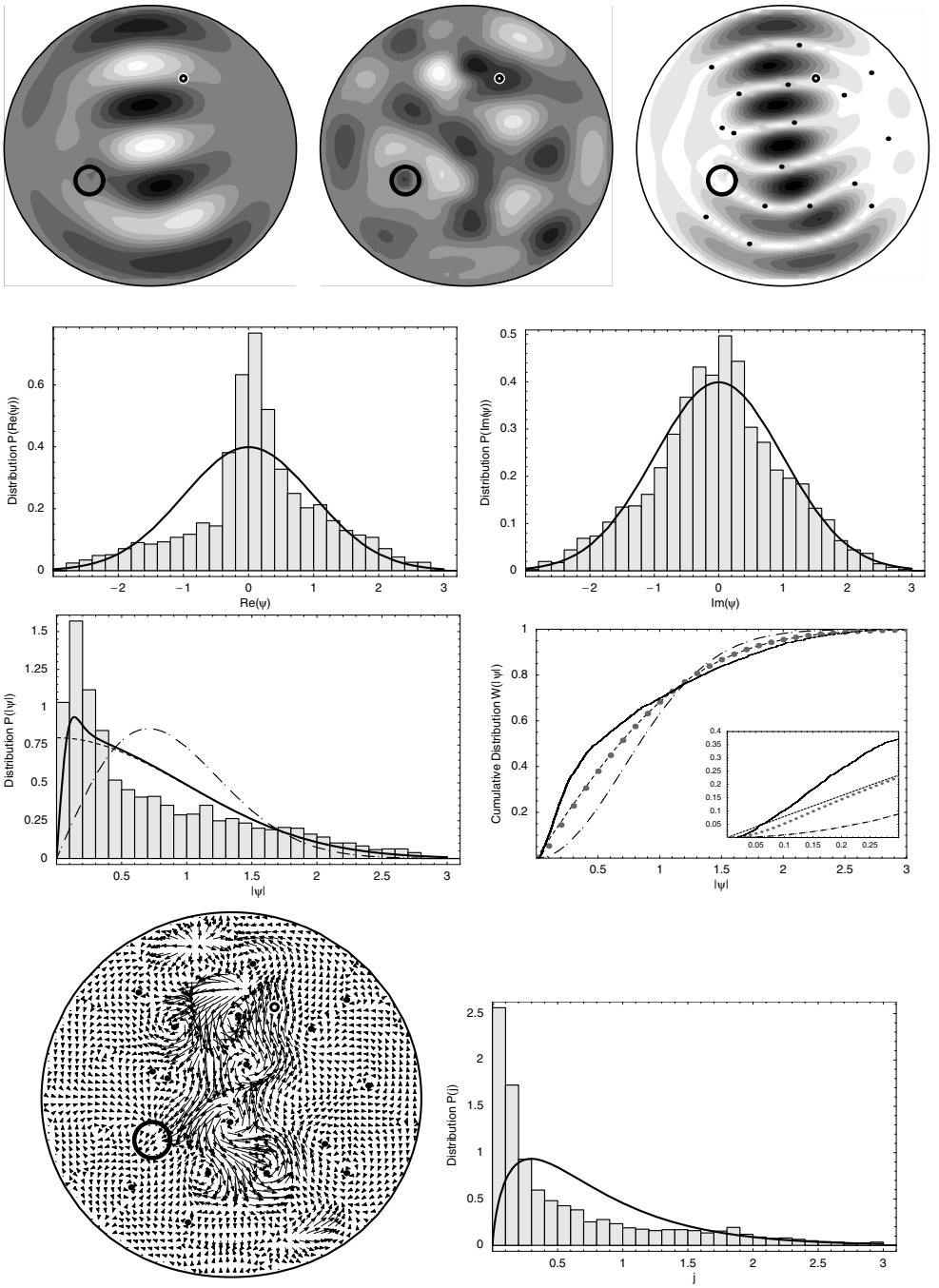

Figure 5. Same as in figure 2 but for the eigenstate of the $\lambda = 0.15$ quadratic billiard corresponding to the $\nu \approx 4.35$ GHz with $\gamma = 0.078$ ($\delta = 0.155$).

probability 1 and the distributed objects are rescaled such that the second moments are 1. In addition to the experimentally obtained distributions the theoretical predictions are plotted as

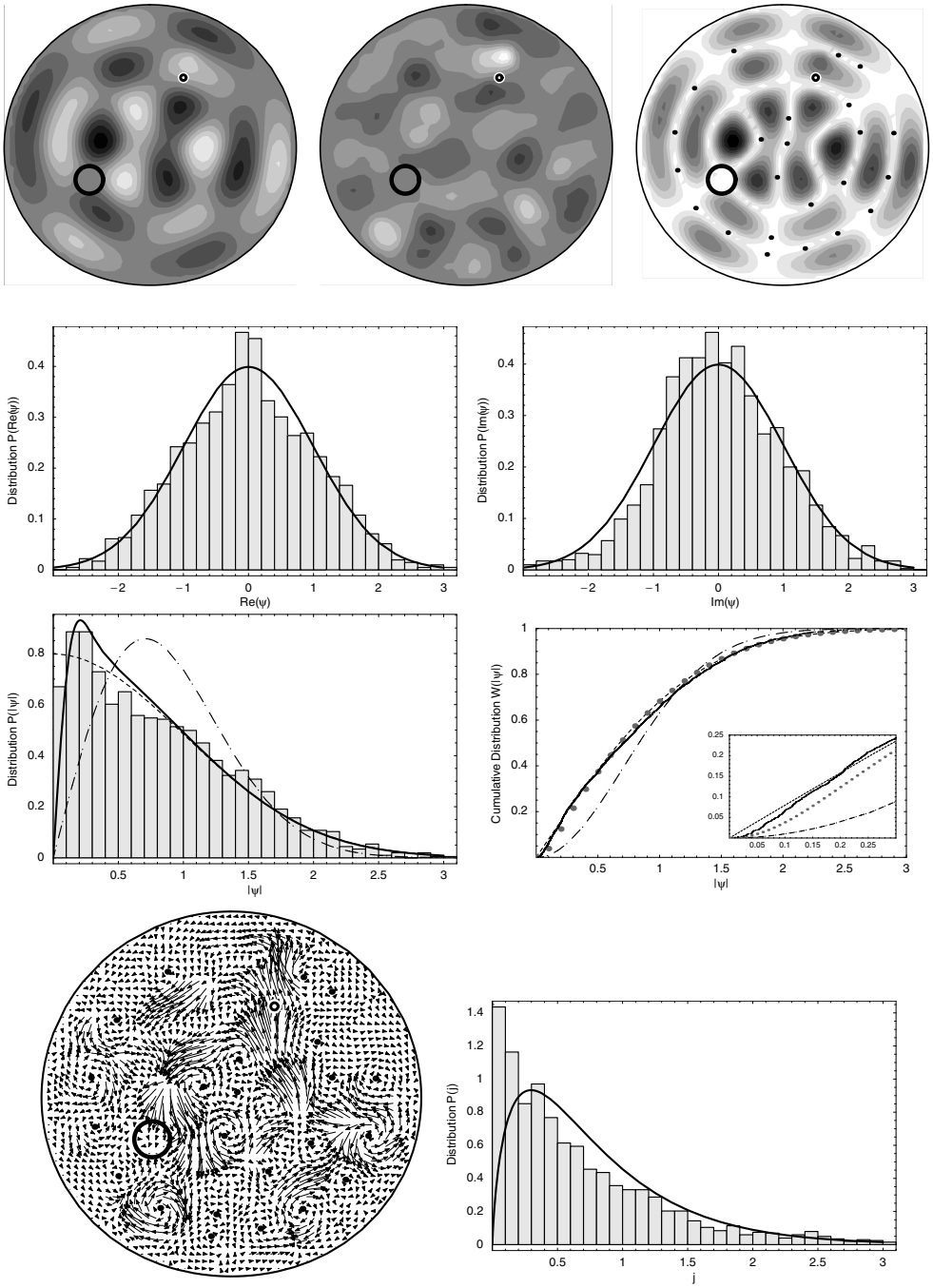

Figure 6. Same as figure 5 but for the billiard eigenstate at $\nu \approx 4.75$ GHz with $\gamma = 0.123$ ($\delta = 0.242$).

thick lines in the histograms of $\mathrm{Re}(\psi)$, $\mathrm{Im}(\psi)$, and $|\psi|$, and with grey bullets in the cumulative distribution of $|\psi|$. In the case of the amplitude $|\psi|$ statistics the non-universal intermediate

distribution (32) is drawn for the values of γ that we calculate from the experimental data according to the definition (29). For comparison the two limiting distributions of $|\psi|$ are drawn as well for the cases (34) and (35) as dashed (GOE) and dashed-dotted (GUE) lines, respectively. The large and the small circles both in the wavefunction's contour plots and in the probability density current vector field plots denote the ferrite ring and the fixed antenna, respectively. The black bullets in the $|\psi|$ and the current plots mark the positions of some of the best visible nodal points of the wavefunction appearing at the same positions as the current vortices.

The three states of the $\lambda = 0.4$ billiard at the resonant frequencies $\nu \approx 4.5$ GHz, $\nu \approx 3.62$ GHz and $\nu \approx 3.45$ GHz in figures 2–4 are sorted in order of decreasing TRS breaking parameter γ (or δ) whose values for the three eigenstates are 0.254 ($\delta = 0.477$), 0.174 ($\delta = 0.338$) and 0.090 ($\delta = 0.179$), respectively. The existence of the non-vanishing imaginary part of the wavefunctions already suggests that TRS of the $\lambda = 0.4$ billiard is broken. Since $\gamma \ll 1$ for all analysed resonances the TRS breaking effect is small but significant, and observable as well in the wavefunction's amplitude distribution which is depressed to 0 as $|\psi| \to 0$ in contrast to the GOE case as is evident from figures 2–4. As already discussed in the previous section the reason for only a small TRS breaking effect can be found in the fact that the studied states lie far below the semiclassical limit in our billiard system. Nevertheless, in particular the distributions and the cumulative distributions of $|\psi|$ displayed in the middle part of the figures show a particularly good agreement with the theoretical predictions even if the γ parameter is extremely small as is the case for the state in figure 4.

For the current distributions shown in the lower right parts of figures 2–4 the correspondence with theory is less pronounced. In all examples there is an overestimation of the small currents, probably arising from the fact that for pixels where the amplitude ψ is close to zero, a reliable determination of the current is no longer possible.

However, we want to understand also a physical source of the experimental error spoiling the topology of the probability density currents in some regions of the billiard. As can be seen from the current vector field plots in the lower left parts of figures 2–4 there are regions of divergent leaking currents which cannot exist in the closed systems. Moreover, these currents cannot exist at many different billiard regions at the same time even when the system is partially open only through the two antennas at two positions, since the waves clearly cannot enter or exit the billiard at regions where no antenna, absorber or other kind of source is present. Similar but much more pronounced divergent currents completely screening the general vortex structure of our results have also been observed by Barth and Stöckmann (2002) where the probability density currents of partially open systems were studied. These anomalies feature most prominently when the neighbouring resonances start to overlap which means that their width is comparable to their spacing. In this case the wavefunctions cannot be successfully resolved any longer by using the simple model described in section 2, because the basic assumptions used in its derivation are no longer fulfilled (see Kuhl *et al* 2000). So, the resulting experimental states that we get by a naive application of the present model in the case of overlapping resonances are in fact mixtures of the true eigenstates. Thus, a more realistic model is required in this case to suppress or/and to unfold the mixing. It is worthwhile mentioning at this point that even when the contribution of two eigenstates is considered to dominate in the Green function (2) at the given frequency, the scattering matrix (5) retains its structure of two superimposed Lorentzian curves (9) but their parameters are now related to both wavefunctions in a nontrivial way.

As described in section 2, the width of the resonances and their spacing depend on the positions of the moving antennas which means that for some eigenstates the mixing is appreciable only at some parts of the billiard domain with the joint measure much smaller than

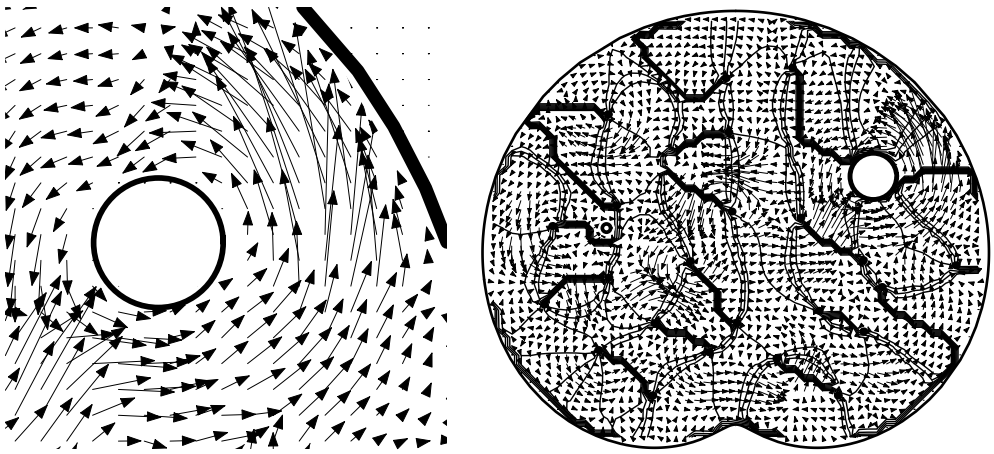

Figure 7. The left part shows a detail of figure 2 in the neighbourhood of the ferrite. The contour plot in the right part of the figure reflects the phase of the eigenfunction, plotted with contours spaced by $\frac{\pi}{4}$. The thick lines correspond to jumps between phase 2π and 0.

the whole billiard area. In these cases the current vector field plots and the wavefunctions are spoiled only locally at these problematic regions which should not spoil our statistical results significantly.

Nothing has been said about the microwave absorption in the ferrite ring so far. To examine this a quadratic box of side length a was placed around the ferrite and the Poynting vector was integrated around the box

$$j_{\mathrm{ab}} = \frac{\oint_{\mathrm{box}} \boldsymbol{P} \cdot \mathrm{d}\boldsymbol{S}}{\oint_{\mathrm{box}} \mathrm{d}S} \tag{38}$$

using the grid data and taking the surface normal vector pointing into the box. The quantity

$$Q = \frac{j_{\mathrm{ab}}}{\sqrt{\langle P^2 \rangle_{\mathrm{box}}}} \qquad \langle P^2 \rangle_{\mathrm{box}} = \frac{\oint_{\mathrm{box}} P^2 \,\mathrm{d}\,S}{\oint_{\mathrm{box}} \mathrm{d}\,S} \tag{39}$$

is defined to compare the average absorptive currents to the magnitude of the total currents at the box considered. The size a of the box was varied from 4 to 10 cm in 1 cm steps and the average value of Q for the three resonances from the figures 2–4 is $\bar{Q} = 0.100$, $\bar{Q} = 0.313$ and $\bar{Q} = 0.441$, respectively. According to these results we can say that the existence of complex wavefunctions and thus non-vanishing probability currents is not predominantly caused by the absorption in the ferrite ring. At least in the case of the first and the second states that we present in figures 2 and 3 the absorptive current can be considered as relatively small due to the small values of $\bar{Q}$. The third resonance shows the strongest absorption of all resonances we analysed and its absorptive current is already comparable in size to the one caused by the boundary reflection effect of the ferrite.

In figure 2 the 'persistent currents' can even be seen directly by eye. As an illustration the left part of figure 7 shows a detail of figure 2 in the neighbourhood of the ferrite. The 'persistent current' manifests itself as a vector field structure encircling the ferrite cylinder. The right part of figure 7 shows the contours of constant phase (spaced by $\frac{\pi}{4}$) of the eigenfunction superimposed on the complete current pattern. From the contour plot it is immediately evident that the 'persistent current' surrounding the ferrite cylinder corresponds to a rotation of the eigenfunction phase of 4π.

We now turn to the discussion of the results for the $\lambda = 0.15$ quadratic billiard. Its classical dynamics is of a mixed type, as mentioned, and so the available phase space consists of regular and chaotic components. As shown by Veble *et al* (2000) the majority of its eigenstates with their energy corresponding to the microwave frequencies from 3 GHz to 5 GHz are localized in the vicinity of the shortest stable or unstable periodic orbits. Such kinds of states are clearly not expected to possess the statistical properties predicted for the irregular chaotic states that we studied before. In figure 5 we show an example of a perturbed regular state at frequency $\nu = 4.35$ GHz whose probability density is localized along the vertical stable periodic orbit still very similar to the case of the empty billiard (see Veble *et al* 2000). Under the action of the ferrite perturbation a small ($\gamma = 0.078$) imaginary part is born giving rise to the non-vanishing probability currents as shown in the lower left part of figure 5. The interesting result is the non-localized structure of the wavefunction's imaginary part reflected in the almost Gaussian distribution of $\mathrm{Im}(\psi)$, which is predicted for chaotic states.

Eigenstates of the empty $\lambda = 0.15$ billiard with a structure similar to that of the real part of the wavefunction such as shown in figure 6 have also been found previously (Veble *et al* 2000). Although we are still far below the semiclassical limit ($\nu = 4.75$ GHz) the phase space objects supporting the Wigner functions of such states can be related to the chaotic components of the corresponding classical phase space, but are localized there. Thus, the (rough) agreement of the histograms in figure 6 with the theoretical curves predicted for the wavefunctions of chaotic systems is not that surprising. However, the deviations can be seen in particular at small values of the amplitudes in the cumulative distribution of $|\psi|$ plotted in figure 6. One reason for the observed discrepancies may be found in the fact that the chaotic components do not extend through the complete available phase space (energy surface) of the $\lambda = 0.15$ billiard. In the semiclassical limit extended chaotic eigenstates supported by a classical chaotic region (smaller than the entire energy surface) are only locally Gaussian random functions, so that the global distributions $P(\mathrm{Re}(\psi))$ and $P(\mathrm{Im}(\psi))$ deviate significantly from the Gaussian case (Berry 1977), and in the case of the systems with TRS also the ψ-autocorrelation function deviates from Berry's function $J_0(ks)$ (Veble *et al* 1999), where J_0 is the Bessel function of order 0, $k = \sqrt{E}$ is the wavenumber and s the distance between the two points in the billiard plane. The absorbing fractions Q of the current, defined above (see equation (39)), are $\bar{Q} = 0.242$, and $\bar{Q} = 0.128$ for the two considered states of the $\lambda = 0.15$ billiard, respectively. Therefore, again we can say that the TRS was partially broken due to the peculiar feature of the ferrite boundary reflection dominating over the microwave absorption effects at least in the case of the states we present in figures 5 and 6.

5. Conclusions

Wavefunctions and probability density currents of two selected quadratic billiards with broken time-reversal symmetry (TRS) have been studied in microwave resonators with a ferrite ring inserted. Such experimental studies are made possible by the exact correspondence between the two-dimensional billiard Schrödinger equation and the electromagnetic wave equation in a quasi-two-dimensional microwave resonator, as well as by the correspondence of the probability density current and the Poynting vector. Since complex-valued wavefunctions are found yielding non-vanishing probability density currents we conclude that TRS is really broken. Due to the fact that far below the semiclassical limit even the chaotic states are not yet completely extended over the billiard domain, the TRS breaking effect is only partial in the sense that the real and imaginary parts of the wavefunctions are not equally strong in the mean. A considerably good agreement between the theory and the experiment is observed in various wavefunction statistics we studied in the chaotic $\lambda = 0.4$ quadratic billiard. Although

the information on wavefunction amplitudes $|\psi|$ in principle can also be extracted from the reflection $\mathcal{S}_{1,1}$ signal the accuracy is vastly improved when the same information is extracted from the transition $\mathcal{S}_{2,1}$ signal. Please note that the analysis of the fully complex information about the transition signal is required to separate the wavefunction's real and imaginary parts and to compute probability density currents.

The agreement between the experiment and the theory can also be observed in the asymptotic tails of the absolute current distribution, while at small currents the discrepancies caused by the experimental error are clearly seen in our results. The unavoidable absorption of microwaves in the ferrite material was also checked to assure that the complex-valued wavefunctions are predominantly formed by the ferrite boundary reflection effect and not by the dissipative microwave absorption.

Acknowledgments

This work was supported by the Ministry of Education, Science and Sport of the Republic of Slovenia and by the Rector's fund of the University of Maribor, as well as by the Deutsche Forschungsgemeinschaft via individual grants. We further gratefully acknowledge the strong support by the scientific and academic cooperation programme between the universities of the twin towns Maribor and Marburg. Finally, the substantial sponsoring financial support by the Nova Kreditna Banka Maribor is gratefully acknowledged.

References

Aharonov Y and Bohm D 1959 *Phys. Rev.* **115** 485
Barth M and Stöckmann H-J 2002 *Phys. Rev.* E at press
Berry M V 1977 *J. Phys. A: Math. Gen.* **10** 2083
Berry M V and Robnik M 1986a *J. Phys. A: Math. Gen.* **19** 649
Berry M V and Robnik M 1986b *J. Phys. A: Math. Gen.* **19** 1365
Dullin H and Bäcker A 2001 *Nonlinearity* **14** 1673
Haake F, Kuś M, Šeba P, Stöckmann H-J and Stoffregen U 1996 *J. Phys. A: Math. Gen.* **29** 5745
Kanzieper E and Freilikher V 1996 *Phys. Rev.* B **54** 8737
Kuhl U, Persson E, Barth M and Stöckmann H-J 2000 *Eur. Phys. J.* B **17** 253
Lax B and Button K J 1962 *Microwave Ferrites and Ferrimagnetics* (New York: McGraw-Hill)
Lévy L P, Dolan G, Dunsmuir J and Bouchiat H 1990 *Phys. Rev. Lett.* **64** 2074
Baowen Li and Robnik M 1994a *J. Phys. A: Math. Gen.* **27** 5509
Baowen Li and Robnik M 1994b unpublished
Markarian R 1993 *Nonlinearity* **6** 819
McDonald S and Kaufman A 1979 *Phys. Rev. Lett.* **42** 1189
McDonald S and Kaufman A 1988 *Phys. Rev.* A **37** 3067
Mohanty P 1999 *Ann. Phys., Lpz.* **8** 549
Narevich R, Prange R E and Zaitsev O 2001 *Physica* E **9** 578
Rehfeld H, Alt H, Dembowski C, Gräf H D, Hofferbert R, Lengeler H and Richter A 1999 *Nonlinear Phenomena in Complex Systems (Minsk)* **2** 44
Richter A 1999 *Emerging Applications of Number Theory, The IMA Volumes in Mathematics and its Applications* vol 109 ed D A Hejhal *et al* (New York: Springer) pp 479–523
Robnik M 1984 *J. Phys. A: Math. Gen.* **17** 1049
Robnik M 1986 *Quantum Chaos and Statistical Nuclear Physiscs (Lecture Notes in Physics vol 263)* ed H T Seligman and H Nishioka (Berlin: Springer) pp 120–30
Robnik M and Berry M V 1986 *J. Phys. A: Math. Gen.* **19** 669
Robnik M *et al* 1983 *J. Phys. A: Math. Gen.* **16** 3971
Saichev A I, Ishio H, Sadreev A F and Berggren K F 2002 *J. Phys. A: Math. Gen.* **35** L87 (nlin.CD/0111010)
Schanze H *et al* 2002 unpublished
Šeba P, Kuhl U, Barth M and Stöckmann H-J 1999 *J. Phys. A: Math. Gen.* **32** 8225
Šeba P, Haake F, Kuś M, Barth M, Kuhl U and Stöckmann H-J 1997 *Phys. Rev.* E **56** 2680

So P, Anlage S M, Ott E and Oerter R N 1995 *Phys. Rev. Lett.* **74** 2662
Soohoo R F 1960 *Theory and Application of Ferrites* (Englewood Cliffs, NJ: Prentice-Hall)
Sridhar S 2000 *Phil. Mag.* B **80** 2129
Sridhar S, Hogenboom D O and Willemsen B A 1992 *J. Stat. Phys.* **68** 239
Stein J, Stöckmann H-J and Stoffregen U 1995 *Phys. Rev. Lett.* **75** 53
Stöckmann H-J 1999 *Quantum Chaos: An Introduction* (Cambridge: Cambridge University Press)
Stöckmann H-J and Stein J 1990 *Phys. Rev. Lett.* **64** 2215
Stoffregen U, Stein J, Stöckmann H-J, Kuś M and Haake F 1995 *Phys. Rev. Lett.* **74** 2666
Veble G, Kuhl U, Robnik M, Stöckmann H-J, Liu J and Barth M 2000 *Prog. Theor. Phys. Suppl.* **139** 283
Veble G, Robnik M and Liu J 1999 *J. Phys. A: Math. Gen.* **32** 6423
Wu D H, Bridgewater J S A, Gokirmak A and Anlage S 1998 *Phys. Rev. Lett.* **81** 2890